Oxidoreductases |*Hot Paper*|

Engineering of Laccase CueO for Improved Electron Transfer in Bioelectrocatalysis by Semi-Rational Design

Lingling Zhang,*[a] Haiyang Cui,[a] Gaurao V. Dhoke,[a] Zhi Zou,[a, b] Daniel F. Sauer,[a] Mehdi D. Davari,[a] and Ulrich Schwaneberg*[a, b]

Abstract: Copper efflux oxidase (CueO) from *Escherichia coli* is a special bacterial laccase due to its fifth copper binding site. Herein, it is discovered that the fifth Cu occupancy plays a crucial and favorable role of electron relay in bioelectrocatalytic oxygen reduction. By substituting the residues at the four coordinated positions of the fifth Cu, 11 beneficial variants are identified with $\geq$2.5-fold increased currents at −250 mV (up to 6.13 mA cm^{-2}). Detailed electrocatalytic characterization suggests the microenvironment of the fifth Cu binding site governs the electrocatalytic current of CueO. Additionally, further electron transfer analysis assisted by molecular dynamics (MD) simulation demonstrates that an increase in localized structural stability and a decrease of distance between the fifth Cu and the T1 Cu are two main factors contributing to the improved kinetics of CueO variants. It may guide a novel way to tailor laccases and perhaps other oxidoreductases for bioelectrocatalytic applications.

Introduction

Laccases (*p*-diphenol:dioxygen oxidoreductase, EC 1.10.3.2), a class of multicopper oxidase, are widely distributed among eukaryotes and prokaryotes.[1] Most laccases contain four Cu atoms per laccase molecule, one Type 1 (T1) Cu and a trinuclear Cu cluster comprised of Type 2 and binuclear Type 3 (T2/T3) Cu atoms. These four Cu atoms participate in intramolecular electron transfer during biocatalysis. The T1 Cu active site accepts four electrons of substrate oxidation and passes them to T2/T3 Cu cluster, where molecular oxygen is fully reduced to two water molecules by accepting four electrons.[2] Copper efflux oxidase (CueO) from *Escherichia coli* belongs to the family of laccase, but it is quite special. CueO laccase has a fifth copper binding site, which is in 7.5 Å distance from the T1 Cu active site.[3] Crystal structure determination shows that the additional Cu binding site is coordinated through two methionines (M355 and M441), two aspartic acids (D360 and D439) and a water molecule in a distorted trigonal bipyramidal geometry. Among them, D439 forms hydrogen bonds with one ligand of the T1 Cu, H443. In addition, CueO possesses an extra 42 amino acid "segment", which lies over the fifth Cu binding site and covers the substrate entrance to the T1 Cu active site. Since this segment is largely helical and includes 14 methionines, it is also referred to as Met-rich helix. M355 and D360 lie at the head and in the middle of the longest helix, respectively.[4] From the view of function, CueO plays an essential role in the copper regulatory system of *Escherichia coli*.[5] It oxidizes extremely toxic Cu^{I} to less toxic Cu^{II} in the periplasm under aerobic conditions.[6]

Unlike most laccases, the oxidase activity of CueO towards common phenolic substrates depends severely on "extra" copper regulation. In 2001, Kim and his co-workers demonstrated that Cu ion addition could stimulate the phenoloxidase and ferroxidase activities of CueO.[7] Grass et al. found that CueO oxidized 2,6-dimethoxyphenol (2,6-DMP) and 2,2′-azinobis(3-ethylbenzothiazoline-6-sulphonic acid) (ABTS) only in the presence of supplemented Cu ions. Without supplemented Cu ions no detectable oxidation of 2,6-DMP and a reduced oxidation rate of ABTS were observed.[5a] After X-ray crystallographic structure determination, Montfort's group confirmed the existence of a labile Cu atom (i.e., the fifth Cu) in CueO and performed site-directed mutagenesis at four coordinated positions. All these four variants (M355L, D360A, D439A, and M441L) led to significantly reduced CueO oxidase activity in vitro towards substrates like 2, 6-DMP and destroyed CueO's copper tolerance in vivo.[3] The latter findings uncovered the important function of the fifth Cu in CueO's catalysis regulation. In the further process of understanding the metabolic mechanism and function of CueO in vivo, Singh et al. proposed

[a] Dr. L. Zhang, H. Cui, Dr. G. V. Dhoke, Dr. Z. Zou, Dr. D. F. Sauer, Dr. M. D. Davari, Prof. U. Schwaneberg
Institute of Biotechnology, RWTH Aachen University
Worringer Weg 3, 52074 Aachen (Germany)
E-mail: l.zhang@biotec.rwth-aachen.de
u.schwaneberg@biotec.rwth-aachen.de

[b] Dr. Z. Zou, Prof. U. Schwaneberg
DWI Leibniz-Institute for Interactive Materials
Forckenbeckstrasse 50, 52074 Aachen (Germany)

Supporting information and the ORCID identification number(s) for the author(s) of this article can be found under: https://doi.org/10.1002/chem.201905598.

that the oxidase activity of CueO is actually a cuprous oxidase activity.[6a] Concretely, Cu^{I} is the only and intrinsic substrate of CueO and it is oxidized at the exact site where the fifth Cu atom lies. The oxidation of other laccase substrates happens in an indirect manner by reducing Cu^{II} at the fifth copper binding site to Cu^{I} and then Cu^{I} is catalyzed by CueO to Cu^{II}.

Laccase-catalyzed oxygen reduction at the electrode has drawn more and more attention in biofuel cell applications in recent decades due to the high electron utilization efficiency (4-electron reduction to water completely).[8] It was reported that direct-electron-transfer (DET)-type bioelectrocatalysis could be readily achieved within CueO.[9] In this context, CueO holds great prospect as a cathodic electrocatalyst in biofuel cells. Considering its unfavorable redox potential in bioelectrocatalysis, we recently reported a successful directed evolution campaign which yielded significantly improved CueO variants.[10] Likewise, it is of high possibility to achieve improved kinetics via directed evolution. In previous CueO engineering reports, many positions located around the first and second spheres of the T1 and T2/T3 Cu sites (i.e., Tyr69,[11] D112,[12] Cys138,[11] Trp139,[11] D439,[13] P444,[13b] Tyr496,[11] C500,[6a] E506,[12b] and M510[13a]) have been mutated. Kataoka et al. have even deleted the extra Met-rich region in order to promote the catalytic activity.[13b,14] Unfortunately, these engineering did not favor the kinetics of electrocatalytic oxygen reduction (except D439A), despite that oxidase activities of some variants were improved. Therefore, it is reasonable to speculate that engineering in the vicinity of the T1 or T2/T3 Cu centers is not promising.

In the present work, we discover the fifth Cu occupancy in CueO plays an important role in bioelectrocatalytic oxygen reduction. In order to acquire highly active variants, site-saturation mutagenesis was performed at four coordinated positions of the fifth Cu (Scheme 1) and the generated library was screened by employing a developed electrochemical screening setup.[10] The obtained beneficial variants verify the effect of the fifth Cu coordination on modulating electrocatalytic kinetics. Furthermore, MD simulations were performed to elucidate possible reasons for improvements. Intramolecular electron transfer was analyzed according to the Marcus theory. These findings provide a new insight in metalloenzyme catalysis besides the well-identified metal active sites and gives useful information for better understanding of the catalytic mechanism of CueO.

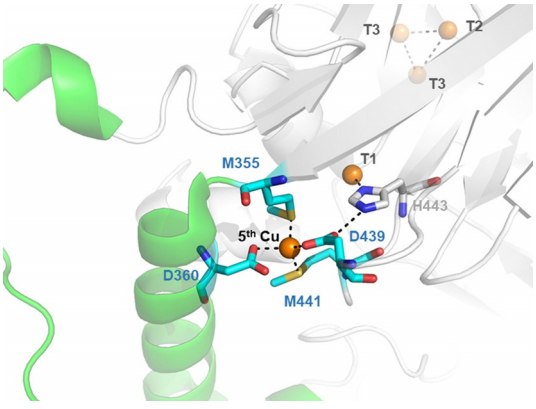

Scheme 1. The structure of CueO (derived from PDB 3OD3) with the fifth Cu coordinated by residues M355, D360, D439, and M441.

Results and Discussion

Although numerous results validated that the existence of the fifth Cu is of crucial importance for CueO to exhibit oxidase activity towards electron-donating substrates, little attentions has been paid to how the fifth Cu electrocatalytically affects CueO-catalyzed oxygen reduction. To the best of our knowledge, only one study mentioned that the presence of additional $CuSO_4$ gave an identical catalytic wave to that in the absence of $CuSO_4$.[9] In the present work, we observed a varied electrocatalytic activity of CueO with and without supplemented Cu^{2+} ions (Figure 1). Curve b was obtained in the circumstance when CueO was expressed according to a commonly used expression protocol for metalloenzymes. 1.5 mM Cu^{2+} ions were supplemented once during the expression. The Cu content was determined by atomic absorption spectroscopy as approx. four atoms per CueO molecule,[12a] implying the occupancy of T1, T2 and two T3 Cu active sites and the vacancy of the fifth Cu binding site. CueO involved in curve c was acquired with supplemented Cu^{2+} ions at the step of cell disruption, which ensured sufficient availability of Cu^{2+} ions to occupy the fifth Cu binding site. Apparently, the peak current density in curve c reaches 0.65 mA cm^{-2}, 7.2-fold higher than the current at 200 mV in curve b, leading to the suggestion that Cu^{2+} occupancy of the fifth Cu binding site remarkably promotes the electrocatalytic activity of CueO towards oxygen reduction. The notably different influences of the fifth Cu on CueO electrocatalysis between the present work and the reported one[9] may be attributed to different electrochemical configurations, especially, different working electrodes. Compared to pyrolytic graphite, hydrophobic CNT is likely able to orient CueO molecules in a favorable conformation on the electrode due to the hydrophobic interaction with the Met-rich region of Cu.[10] In this conformation, the fifth Cu atom underneath the Met-rich region is closer to the electrodes, thus exerting evidently its intramolecular electron-mediating role.

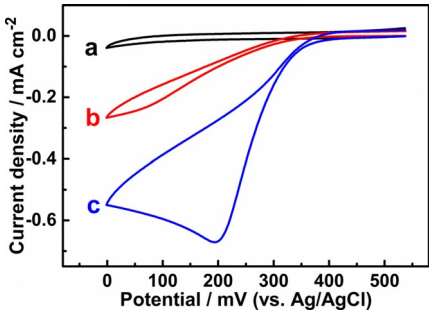

Figure 1. Cyclic voltammograms (CVs) obtained at different modified carbon nanotubes/glassy carbon (CNT/GC) electrodes in air-saturated NaAc-HAc buffer (0.1 M, pH 5.5): blank lysate with supplemented $CuSO_4$ (a), CueO lysate without (b) and with (c) extra $CuSO_4$ addition. Scan rate is 10 mV s^{-1}.

The fifth Cu of CueO is structurally coordinated by four ligands, M355, D360, D439, and M441. For the sake of seeking variants of higher electrocatalytic activity towards oxygen reduction as well as understanding the possible electrocatalytic mechanism, SSM was performed at these four positions. The generated CueO library were screened via the previously developed electrochemical screening platform.[10] The current values at 0 mV were set as the evaluation criterion. Consequently, 11 beneficial variants (M355A, M355I, M355L, D360K, D360S, D439A, D439H, D439T, D439V, M441H, and M441V) were identified. It indicates all these four coordinated positions of the fifth Cu are important for maintaining the electrocatalytic activity of CueO and tuning its electrocatalytic kinetics via protein engineering.

Rotating disk electrode (RDE) was employed to study and compare the electrocatalytic kinetics of the 11 CueO beneficial variants as well as CueO WT. The comparison is based on the saturated CueO adsorption on CNT/GC electrodes. SDS-PAGE characterization (Figure S1) combined with enzyme quantification demonstrate that the CueO variants are expressed at comparable concentrations ranging from 120 to 140 μM. Notably while 20 μM proved to be sufficient for a maximal catalytic current according to the previously reported results.[10] Figure 2A shows the rotating disk voltammograms of CueO WT (A) and four representative CueO variants (B to E: M355A, D360K, D439T, and M441H). It is clear that the electrocatalysis of CueO D360K produces the largest catalytic current at −250 mV, reaching 6.13 mA cm^{-2}. It is approximately 4.38 times higher than that of CueO WT (1.40 mA cm^{-2}). M355A, D439T and M441H show 4.09, 3.95, and 2.64-fold improved catalytic current at −250 mV, respectively. To quantify the improved factors of four CueO variants, Tafel slopes was plotted and fitted linearly according to the Tafel equation ($\eta = a + b \log|j|$, where j is the current density and b is the Tafel slope) based on the corresponding polarization curves in Figure 2A. Tafel slope represents how fast the overpotential goes up with the current density and a kinetics-favorable electrochemical reaction should exhibit a low Tafel slope.[15] As shown in Figure 2B, the values of Tafel slopes were estimated as −111, −70, −62, −61, and −77 mV dec^{-1} for CueO WT, M355A, D360K, D439T, and M441H, respectively. Obviously, the absolute values of all four CueO variants are lower than that of CueO WT, especially D360K with the lowest the slope of −61 mV dec^{-1}, indicating more favorable kinetics.

Table 1. Electrocatalytic parameters of CueO WT and beneficial variants at four coordinated positions of the fifth Cu binding site.

Enzyme	Current at −250 mV [mA cm^{-2}]	Relative current	Tafel slope [mV dec^{-1}]
CueO WT	1.40 ± 0.12	1.00	−111 ± 3
CueO M355A	5.72 ± 0.09	4.09	−70 ± 2
CueO M355I	5.47 ± 0.14	3.91	−71 ± 3
CueO M355L	5.36 ± 0.26	3.83	−73 ± 2
CueO D360K	6.13 ± 0.15	4.38	−62 ± 3
CueO D360S	5.45 ± 0.23	3.89	−63 ± 3
CueO D439A	5.57 ± 0.04	3.98	−61 ± 2
CueO D439H	5.42 ± 0.04	3.87	−61 ± 3
CueO D439T	5.53 ± 0.13	3.95	−61 ± 2
CueO D439V	5.62 ± 0.21	4.01	−61 ± 2
CueO M441H	3.69 ± 0.23	2.64	−77 ± 1
CueO M441V	3.58 ± 0.27	2.56	−77 ± 1

Three parallel measurements were carried out for each enzyme.

Table 1 gives an overview of the electrocatalytic properties for all the beneficial variants. Obviously, all the CueO variants present higher currents and lower absolute values of Tafel slopes than CueO WT, confirming the reliability of the screening system and suggesting the proximal positions of the fifth Cu play a key role in electrocatalysis manipulation. It is worth noting that substitutions of D439, which was reported to shift the onset potential to a higher potential,[10] could also contribute to the catalytic current. The present result reinforces and complements the former explanation. Position 439 is adjacent to a coordinated ligand of the T1 Cu active site, meanwhile, it lies in the electron-transfer pathway from electrode to the T1 Cu site. The former affects the onset potential and the latter influences the catalytic current. As the fifth Cu may act as an electron relay in the electron-transfer pathway between the electrode and the T1 Cu active site,[9] the electrons from the electrode first go to the fifth Cu binding site due to a favorable orientation of CueO on the electrodes. After that, the electrons reach the T1 Cu active site via the electron-transfer pathway comprising the proximal residue 439 and H443. In the cases of the other three proximal positions (355, 360 and 441), they make little impact on the T1 Cu active site and thereby have

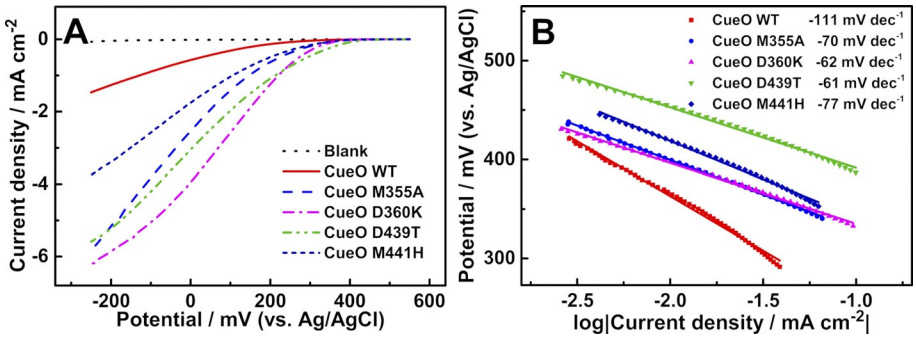

Figure 2. Rotating disk voltammograms (A) and the corresponding Tafel plots (B) of oxygen reduction catalyzed by CueO WT and four CueO variants immobilized on CNT/GC electrodes in O_2-saturated NaAc-HAc buffer (0.1 M, pH 5.5) at a scan rate of 5 mV s^{-1}.

no influence on onset potential. Accordingly, it can be concluded, like the T1 Cu dominates the redox potential (thermodynamics), the fifth Cu partially governs the electrocatalytic kinetics of CueO. Based on these beneficial variants, attempts of combination were also made between substitutions M355 and D439, as combination is a routine approach to amplify the mutation benefits. Unfortunately, no synergistic enhancements were observed in any double-substituted variants (data not shown). Some of them even exhibited reduced activity than either of the single-substituted variants. The possible reason might be that either two of the positions are close spatially, and two substitutions at the same time would result in severe change of the coordination microenvironment.

Considering the importance of the fifth Cu in CueO electrocatalysis, it is significant to unveil the catalytic mechanism at a molecular level. To the best of our knowledge, the electron transfer at a fifth Cu coordinated by two thioether-S and carboxyl-O ligands has not been reported yet, although electron transfer mechanisms are well understood in various cooper-containing proteins, especially T1 Cu protein azurin.[16] Before implementing the MD simulations, we validated the existence of the fifth Cu in both CueO WT and four CueO variants with inductively coupled plasma-optical emission spectrometry (ICP-OES, Table S2). Apparently, all contain more than five Cu atoms per protein molecule and there are no obvious changes within the Cu contents between CueO WT and the four investigated variants. The slight overrepresentation of the copper content per CueO molecule can possibly be attributed to the several amino acid residues (e.g., like methionine and histidine) on the surface of CueO and may attract more Cu to the vicinity.[4b] MD simulation was performed at the fifth Cu binding region (including Cu atom and the four coordinated ligands). It was found that the time-averaged RMSD decrease for all the four CueO variants compared to CueO WT (Figure 3 A), although the overall structural integrity was maintained (Figures S3 and S4). An increase in localized structural stability is speculated to stabilize productive confirmations and thereby raise the efficiency of electron inflow from the electrode to the fifth Cu binding site.[17] In another aspect, the electrocatalytic kinetics can be studied with Marcus theory, which illustrates that the electron transfer rate between electron donor and acceptor, according to the theory, is determined by the driving force (i.e., the free energy change, $-\Delta G^0$), the distance between two centers, and the reorganization energy (λ).[18] The free energy change (redox potential in electrochemical reaction), except for D439 substitutions, did not show obvious changes between CueO variants and CueO WT. In CueO, intramolecular electron transfer includes two steps: from the fifth Cu binding site to the T1 Cu active site and from T1 Cu to T2/T3 Cu cluster through an amino acid sequence HCH motif. Since the substitutions happen at the fifth Cu binding site, we extracted the distance distribution data from the fifth Cu binding site to the T1 Cu active site in CueO WT and four CueO variants (Figure 3 B). Apparently, the distances decrease from 10.5 Å of CueO WT to 9.3, 7.5, 7.0, and 5.6 Å of CueO D439T, M355A, M441 H, and D360K, respectively, providing strong evidence of accelerated electron transfer in CueO variants. The λ value represents the energy required for ligand and solvent rearrangements between initial and final equilibrium.[19] The possible decline of λ at the fifth Cu region of CueO variants is speculated resulted from two aspects: The increased hydrophobicity and decreased electron-donating ability of primary ligands. Metalloprotein folding study suggested the exclusion of water from the Cu active site and the rigidity of the hydrophobic cavity contributed by the coordinated ligands are important for λ.[20] Kinetics of enzymatically catalyzed redox reactions is very sensitive to the active-site environments. In this circumstance, the improved activities of variants like M355A, M355I, M355L, D439A, D439V, and M441V may be partially caused by the increased hydrophobicity of the fifth Cu center. Secondly, lower electron donating residues (e.g., H, K, T, and S) than M and D would decrease the electron density of the fifth Cu center and elevate its oxidized state, probably enabling a faster electron inflow to the fifth Cu center from the electrode and accelerating electron transfer. As 11 beneficial variants were ascertained, it is likely that multiple modes exist for optimization. For instance, longer bond lengths may weaken the metal–ligand interaction as well as the efficiency of electron-donating/withdrawing.

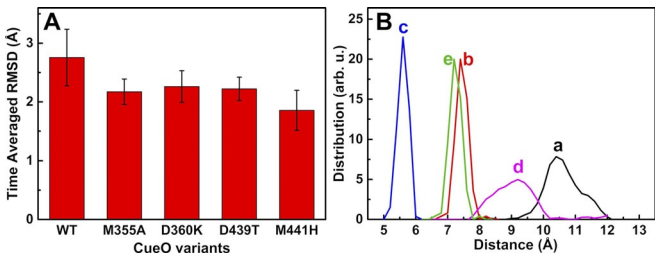

Figure 3. (A) Time-average RMSD of the fifth Cu binding site of CueO WT and variants determined from the last 80 ns simulation. The fifth Cu binding site is defined the Cu atom and the four coordinated ligands. The error bar was calculated from three runs with different starting atomic velocities. (B) Distance distributions curves between the fifth Cu and the T1 copper in CueO WT (a), CueO M355A (b), CueO D360K (c), CueO D439T (d), and CueO M441H (e).

Conclusions

In summary, we have validated the promotion role of the fifth Cu occupancy in bioelectrocatalytic oxygen reduction at CueO/CNT/GC electrodes. Different from the reported results, we have proposed the fifth Cu likely acts as an efficient electron relay by virtue of the favorable conformation induced by hydrophobic CNT with the fifth Cu close enough to the electrode surface. By screening the SSM library of four coordinated positions of the fifth Cu binding site, 11 beneficial variants have been identified with $\geq$2.5-fold increased currents. Rotating disk voltammetric measurements have revealed that the fifth Cu partially governs the electrocatalytic kinetics of CueO. As position 439 connected the fifth Cu binding site and the T1 Cu active site, both the redox potential and catalytic current have got improvements in D439 variants. The results from MD simulation and analysis have suggested that an increase in localized structural stability and a decrease of distance between the fifth

Cu binding site and the T1 Cu active site are the two main factors that contribute to the improved electrocatalytic kinetics of CueO variants. This work provides a new insight in multicopper oxidase catalysis besides the well-identified four Cu active sites and gives some useful hints for better understanding the catalytic mechanism of CueO. Moreover, it inspires more efficient computer-assisted rational design of oxidoreductase for bioelectrocatalytic applications.

Experimental Section

CueO library generation via SSM

Mutations at positions M355, D360, D439, and M441 were introduced by the following primers:

M355_forward: 5′-GCTGCAACTCTCTNNKGACCCGATGCTC-3′

M355_reverse: 5′-GAGCATCGGGTCMNNAGAGAGTTGCAGC-3′

D360_forward: 5′-GACCCGATGCTCNNKATGATGGGGATG-3′

D360_reverse: 5′-CATCCCCATCATMNNGAGCATCGGGTC-3′

D439_forward: 5′-GGCGTGGGCNNKATGATGCTGC-3′

D439_reverse: 5′-GCAGCATCATMNNGCCCACGCC-3′

M441_forward: 5′-GTGGGCGACATGNNKCTGCATCCGTTCCAT-3′

M441_reverse: 5′-ATGGAACGGATGCAGMNNCATGTCGCCCAC-3′

PCR for diversity generation was performed with a modified two-step QuikChange™ Mutagenesis according to our previous procedure.[21] The PCR products were digested with DpnI and purified with commercial kit NucleoSpin Plasmid Extraction. Afterwards, 2 μL of the PCR products were transformed into 100 μL *E. coli* SHuffle® T7 Express competent cells (heat shock at 42 °C for 45 sec) and recovered at 37 °C for 1 h. These cells were plated on LB_{AMP} agar plates for growth overnight at 37 °C. Afterwards, the clones on the plate were transferred to 96-well microtiter plates (MTPs) filled with 150 μL LB_{AMP} medium and cultivated in a MTP shaker for 20 h (37 °C, 900 rpm, 70% humidity). Two MTPs were prepared for each position to ensure a complete coverage of the natural diversity. The MTPs were placed at −80 °C followed by addition of 100 μL glycerol (50% v/v) in each well for long-term storage.

Electrochemical screening

A previous protocol[10] was used to express CueO variants in 96-well MTPs. Basically, 1.5 mM $CuSO_4$ was added in two steps: expression induction and cell disruption. Each ITO electrode in the 8-electrode array was modified with 1 μL of multi-wall carbon nanotubes (CNT, 9.5 nm in diameter, 1.5 μm in length, purity >95%) suspension by drop-casting and the dry CNT/ITO electrode array was immersed into crude enzyme solution in 96-well format for CueO substitution immobilization. A three-electrode configuration was set up with eight working electrodes sharing one reference electrode and one auxiliary electrode. Linear sweep voltammetry with a faster scan rate of 10 mV^{-1} was employed to record eight linear sweep voltammetric curves simultaneously and separately at Dropsens 8-channel potentiosat (μstat 8000P, Spain). The catalytic current values at 0 mV were compared to evaluate the electrocatalytic performances of CueO variants. Twelve measurements repeated to cover a 96-well MTP. After screening and rescreening, the picked beneficial variants were identified by DNA sequencing.

Bioelectrocatalysis of CueO WT and CueO variants

CNT modified glassy carbon electrodes (diameter: 3 mm, geometric area: 0.07 cm^2) were used to characterize the bioelectrocatalytic properties of CueO WT and CueO variants. 10 μL of CNT suspension was drop-cast on a fresh GC electrode, termed as CNT/GC electrode. CNT/GC electrodes were soaked in the respective enzyme lysates for 20 s and then rinsed to remove loosely and nonspecifically binding components. A conventional three-electrode configuration was set up with enzyme attached CNT/GC electrode as working electrode, Ag/AgCl (3 M NaCl) as reference electrode and platinum spiral wire as auxiliary electrode. All the electrochemical measurements in this section were performed on Autolab PGSTAT128N (Metrohm AG, Switzerland).

To investigate the role of the fifth binding Cu in bioelectrocatalysis, cyclic votammograms were recorded within crude enzyme samples of CueO, CueO with insufficient Cu^{2+} binding (**control A**) and blank (**control B**) were prepared. Control A means the crude enzyme solution without supplemented $CuSO_4$ in the step of cell disruption. In control B, a plasmid without CueO insert (empty vector) was transformed into *E. coli* SHuffle® T7 Express competent cells, followed by the same cultivation and expression protocol as for CueO. In this case, blank lysate without CueO expression was obtained.

To characterize electrocatalytic kinetics of the beneficial CueO variants obtained from screening, a rotating disk electrode setup (Metrohm Autolab B. V., Utrecht, the Netherlands) with a compatible glassy carbon electrode mounted on a rotating shaft and a motor controller was used for determining bioelectrocatalytic kinetics. The compatible GC electrode was modified with CNT and CueO variants as described before. Since it has been verified that CueO content in cell lysate is approximately 90% and crude CueO is saturated for its adsorption on electrodes,[10] all the subsequent assays were carried out with crude enzyme solutions. Linear sweep voltammograms were recorded at different rotating speeds after ten rounds of cyclic voltammetric scan to ensure stable and precise determination of kinetics parameters. The scan rate was set to 5 mV^{-1}. Before that, SDS-PAGE characterization of crude enzymes as well as catalytic activity determination was performed to investigate the comparison feasibility of CueO WT and 11 beneficial variants. For the rotating disk voltammetric curves obtained in oxygen-saturated condition, NaAc-HAc buffer (0.1 M, pH 5.5) was purged with high-purity O_2 gas for 20 min and then protected by O_2 atmosphere during recording. Specifically, Tafel slopes of CueO WT, CueO M355A, CueO D360K, CueO D439T, and CueO M441H were acquired according to the corresponding polarization curves (225 rpm, oxygen saturation). For the measurements within dissolved oxygen, NaAc-HAc buffer (0.1 M, pH 5.5) was used directly. The current values at different potentials were picked out for kinetic current study according to the Koutecky–Levich equation.[15]

The Cu contents in CueO WT and four CueO variants (M355A, D360K, D439T, and M441 H) were measured with inductively coupled plasma-optical emission spectrometry (ICP-OES, PlasmaQuant PQ 9000 Elite, Analytik Jena). 2 mL purified enzyme sample were digested with 6 mL HNO_3 (65%) by microwave. Three parallel measurements were repeated for each sample.

Molecular dynamic simulations

The crystal structure of CueO was obtained from the protein data bank (PDB ID: 3OD3).[4b] The fifth copper Cu^{II} was built in CueO structure to generate a completed CueO structure according to the distances between Cu and ligands in CueO C500S crystal structure (PDB ID: 3NT0).[4b] The completed CueO WT structure was

used as the template to generate variants M355A, D360K, D439T, and M441H by YASARA Structure version 13.9.8.[22] The substituted residue was optimized by semi-empirical quantum mechanics. Molecular dynamics (MD) simulation and analysis was performed with GROMACS v5.1.2 software.[23] The ff99SBildn force field was used for the simulation of CueO WT as well as variants. The protonation state of the ionizable residues was defined corresponding to pH 5.5. Structures were solvated into a cubic box of TIP3P water molecules with a minimal distance of the protein to the borders of 1.2 nm. They were filled with around 18000 water molecules in simulation systems.

In all cases, the system was carefully minimized and equilibrated using the following protocol. Step 1, 1000 steps of energy minimization were carried out for protein using steepest descent algorithm, until it converged with a force tolerance of 500 kJ mol^{-1} nm^{-1}. Step 2, 5000 steps of energy minimization were carried out only for solvent molecules with a force tolerance of 250 kJ mol^{-1} nm^{-1} after filling the box with water. Step 3, after minimization, each system was equilibrated to 298 K through a stepwise heating protocol in the NVT ensemble followed by 100 ps equilibration in the NPT ensemble with position restraints on the protein molecule. The production simulation time for all were chosen to be 100 ns at 298 K and 1 bar (timestep of 2 fs) after the proteins were relaxed. To avoid artifacts, the MD simulations were run three times with different starting atomic velocities and one of the three runs is shown as a representative.

Root mean square deviation (RMSD), root mean square fluctuation for each residue (RMSF), and distance distribution were calculated by GROMACS simulation package tools. Pymol was used to visualize the structural change of protein.

Acknowledgements

L.Z. acknowledges the support from the Alexander von Humboldt Foundation. The authors would like to thank Alexander von Humboldt postdoctoral fellow Dr. Kaixuan Chen for the helpful discussion.

Conflict of interest

The authors declare no conflict of interest.

Keywords: bioelectrocatalysis · copper efflux oxidase · electron transfer · oxygen reduction reaction · site-saturation mutagenesis

[1] a) A. M. Mayer, R. C. Staples, *Phytochemistry* **2002**, *60*, 551–565; b) H. Claus, *Micron* **2004**, *35*, 93–96; c) O. V. Morozova, G. P. Shumakovich, S. V. Shleev, Y. I. Yaropolov, *Appl. Biochem. Microbiol.* **2007**, *43*, 523–535.
[2] a) S. Riva, *Trends Biotechnol.* **2006**, *24*, 219–226; b) D. E. Heppner, C. H. Kjaergaard, E. I. Solomon, *J. Am. Chem. Soc.* **2014**, *136*, 17788–17801; c) S. Wherland, O. Farver, I. Pecht, *J. Biol. Inorg. Chem.* **2014**, *19*, 541–554.
[3] S. A. Roberts, G. F. Wildner, G. Grass, A. Weichsel, A. Ambrus, C. Rensing, W. R. Montfort, *J. Biol. Chem.* **2003**, *278*, 31958–31963.
[4] a) S. A. Roberts, A. Weichsel, G. Grass, K. Thakali, J. T. Hazzard, G. Tollin, C. Rensing, W. R. Montfort, *Proc. Natl. Acad. Sci. USA* **2002**, *99*, 2766; b) S. K. Singh, S. A. Roberts, S. F. McDevitt, A. Weichsel, G. F. Wildner, G. B. Grass, C. Rensing, W. R. Montfort, *J. Biol. Chem.* **2011**, *286*, 37849–37857.
[5] a) G. Grass, C. Rensing, *Biochem. Biophys. Res. Commun.* **2001**, *286*, 902–908; b) G. Grass, C. Rensing, *J. Bacteriol.* **2001**, *183*, 2145.
[6] a) S. K. Singh, G. Grass, C. Rensing, W. R. Montfort, *J. Bacteriol.* **2004**, *186*, 7815; b) K. Y. Djoko, L. X. Chong, A. G. Wedd, Z. Xiao, *J. Am. Chem. Soc.* **2010**, *132*, 2005–2015.
[7] C. Kim, W. W. Lorenz, J. T. Hoopes, J. F. D. Dean, *J. Bacteriol.* **2001**, *183*, 4866.
[8] a) N. Mano, A. de Poulpiquet, *Chem. Rev.* **2018**, *118*, 2392–2468; b) A. Le Goff, M. Holzinger, S. Cosnier, *Cell. Mol. Life Sci.* **2015**, *72*, 941–952.
[9] Y. Miura, S. Tsujimura, Y. Kamitaka, S. Kurose, K. Kataoka, T. Sakurai, K. Kano, *Chem. Lett.* **2007**, *36*, 132–133.
[10] L. Zhang, H. Cui, Z. Zou, T. M. Garakani, C. Novoa-Henriquez, B. Jooyeh, U. Schwaneberg, *Angew. Chem. Int. Ed.* **2019**, *58*, 16314–16319; *Angew. Chem.* **2019**, *131*, 16460–16465.
[11] T. Sakurai, M. Yamamoto, S. Ikeno, K. Kataoka, *Biochim. Biophys. Acta Proteins Proteomics* **2017**, *1865*, 997–1003.
[12] a) Y. Ueki, M. Inoue, S. Kurose, K. Kataoka, T. Sakurai, *FEBS Lett.* **2006**, *580*, 4069–4072; b) K. Kataoka, R. Sugiyama, S. Hirota, M. Inoue, K. Urata, Y. Minagawa, D. Seo, T. Sakurai, *J. Biol. Chem.* **2009**, *284*, 14405–14413.
[13] a) Y. Miura, S. Tsujimura, S. Kurose, Y. Kamitaka, K. Kataoka, T. Sakurai, K. Kano, *Fuel Cells* **2009**, *9*, 70–78; b) K. Kataoka, S. Hirota, Y. Maeda, H. Kogi, N. Shinohara, M. Sekimoto, T. Sakurai, *Biochemistry* **2011**, *50*, 558–565.
[14] K. Kataoka, H. Komori, Y. Ueki, Y. Konno, Y. Kamitaka, S. Kurose, S. Tsujimura, Y. Higuchi, K. Kano, D. Seo, T. Sakurai, *J. Mol. Biol.* **2007**, *373*, 141–152.
[15] W. Xia, A. Mahmood, Z. Liang, R. Zou, S. Guo, *Angew. Chem. Int. Ed.* **2016**, *55*, 2650–2676; *Angew. Chem.* **2016**, *128*, 2698–2726.
[16] a) O. Farver, I. Pecht, *Proc. Natl. Acad. Sci. USA* **1989**, *86*, 6968; b) M. Van de Kamp, R. Floris, F. C. Hali, G. W. Canters, *J. Am. Chem. Soc.* **1990**, *112*, 907–908; c) A. R. Bizzarri, C. Baldacchini, S. Cannistraro, *Langmuir* **2017**, *33*, 9190–9200.
[17] a) J. D. Bloom, S. T. Labthavikul, C. R. Otey, F. H. Arnold, *Proc. Natl. Acad. Sci. USA* **2006**, *103*, 5869; b) K. S. Siddiqui, *Crit. Rev. Biotechnol.* **2017**, *37*, 309–322.
[18] a) O. Farver, L. K. Skov, G. Gilardi, G. van Pouderoyen, G. W. Canters, S. Wherland, I. Pecht, *Chem. Phys.* **1996**, *204*, 271–277; b) C. Léger, F. Lederer, B. Guigliarelli, P. Bertrand, *J. Am. Chem. Soc.* **2006**, *128*, 180–187.
[19] L. Paltrinieri, M. Borsari, A. Ranieri, G. Battistuzzi, S. Corni, C. A. Bortolotti, *J. Phys. Chem. Lett.* **2013**, *4*, 710–715.
[20] a) J. R. Winkler, P. Wittung-Stafshede, J. Leckner, B. G. Malmström, H. B. Gray, *Proc. Natl. Acad. Sci. USA* **1997**, *94*, 4246–4249; b) H. B. Gray, B. G. Malmström, R. J. P. Williams, *J. Biol. Inorg. Chem.* **2000**, *5*, 551–559; c) H. B. Gray, J. R. Winkler, *Annu. Rev. Biochem.* **1996**, *65*, 537–561.
[21] W. Wang, B. A. Malcolm, *BioTechniques* **1999**, *26*, 680–682.
[22] E. Krieger, G. Vriend, *Bioinformatics* **2014**, *30*, 2981–2982.
[23] M. J. Abraham, T. Murtola, R. Schulz, S. Páll, J. C. Smith, B. Hess, E. Lindahl, *SoftwareX* **2015**, *1–2*, 19–25.

Manuscript received: December 11, 2019
Revised manuscript received: January 22, 2020
Accepted manuscript online: January 27, 2020
Version of record online: March 18, 2020